

Isoprene hydroamination catalyzed by palladium xantphos complexes

Bahareh Tamaddoni Jahromi^a, Ali Nemati Kharat^{a,*}, Sara Zamanian^a, Abolghasem Bakhoda^b, Kobra Mashayekh^a, Sadegh Khazaeli^b

^a School of Chemistry, University College of Science, University of Tehran, Tehran, Iran

^b Department of Chemistry, Southern Illinois University, Edwardsville, IL 62026, United States

ARTICLE INFO

Article history:

Received 26 February 2012

Received in revised form 11 May 2012

Accepted 14 May 2012

Available online 22 May 2012

Keywords:

Isoprene

Secondary amines

Hydroamination

Palladium complexes

Xantphos

ABSTRACT

Pd(II) Xantphos or Xantphos chalcogenide complexes with general formula $[PdCl_2(X\cap X)]$ (where X = P, O, S or Se) were synthesized by the addition of corresponding ligands to $[PdCl_2(COD)]$ (COD = 1,5-cyclooctadiene). Prepared Complexes $[PdCl_2(Xantphos)]$ and $[PdCl_2(Xantphos=S)]$ showed distorted square planar geometries, from X-ray crystallographic analysis. All of the prepared complexes showed activity toward intermolecular hydroamination of isoprene with a variety of secondary amines. Complete conversion (~100%) of pyrrolidine was observed using Pd–Xantphos as catalysts. Hydroamination reactions exhibited regioselectivity when crowded secondary amines were used.

© 2012 Elsevier B.V. All rights reserved.

1. Introduction

Intermolecular hydroamination, the addition of N–H bond across C=C multiple bonds has recently received great deal of attention because being a 100% atom-economy process. The reaction allows direct access to a large variety of amines which are important target products or intermediates in organic and medicinal chemistry. A number of papers were published [1–10], reporting the hydroamination of alkenes or alkynes and the difference between hydroamination and related oxidative amination reactions. Hydroamination is known to be catalyzed by complexes of early/late transition metals (especially groups IX and X) and some lanthanide complexes [11–15]. The big step in hydroamination of C=C bonds took place at the start of the 21st century when Hartwig and his co-workers published intermolecular reactions of vinylarenes with arylamines using palladium–phosphine systems either with OTf[−] or in the presence of triflic or trifluoroacetic acids as co-catalysts [16]. The addition took place in anti-Markovnikov fashion and strong evidence (computational [17] and experimental [18]) supported the presence of η^3 -phenethyl palladium complex as the intermediate. Pd complexes bearing sterically hindered PXP ligands (where X = C or N) were discovered to catalyze the hydroamination of primary and secondary amines with activated alkenes [19]. Palladium diphosphine complexes were also found to catalyze the hydroamination of secondary alkyl, cycloalkyl

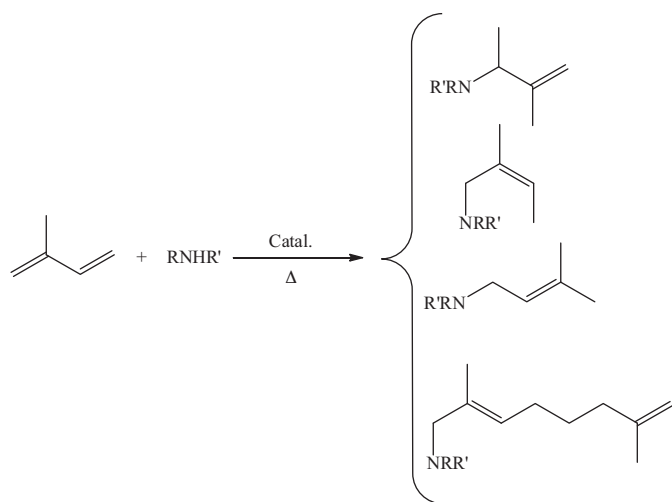
and benzylic amines to acrylic type alkenes [20]. Although the isolated yields were remarkable in most cases, drastic conditions were necessary for the reaction.

Hydroamination of 1,3-dienes with ammonia underlie the promising preparation procedures for higher amines. The most interesting product of butadiene hydroamination with NH₃ is tris(2,7-octadienyl)amine that can be easily hydrogenated to obtain trioctylamine, a valuable extractant extensively applied in isolation processes of a large number of noble and rare metals. In the earlier studies, butadiene hydroamination was performed in the presence of palladium catalyst with triarylphosphine or dialkylarylphosphine oxide ligands, with anhydrous ammonia under high pressure. The product distribution depends on the ratio of butadiene to ammonia and on the character of the solvent, as well as the concentration of NH₃. Hydroamination of isoprene catalyzed by Pd and Ni complexes provides a convenient synthetic method to aminoterpenes [21,22]. Since the isoprene could be coupled in four fashion (head-to-tail, tail-to-head, head-to-head, and tail-to-tail), the composition of the 2:1 adducts of isoprene and amines are usually complex. From the synthetic point of view, the importance of the procedure for the preparation of amino-substituted hemiterpenes and monoterpenes is its selectivity to prenolamine, buteneamines and 3,7-dimethylocta-2,7-dien-1-amine. These compounds are structural elements of a diverse natural isoprenoids [23] (see Scheme 1).

The main factors determining the regioselectivity in the reactions of isoprene with amines are (a) the nature of initial amine, (b) the structure of activating ligand in the catalyst, and (c) the presence of acid co-catalyst (HOTf or BF₃·Et₂O) [24]. The nature

* Corresponding author. Tel.: +98 21 61112499; fax: +98 21 66495291.

E-mail address: alnema@khayam.ut.ac.ir (A. Nemati Kharat).



Scheme 1. Catalytic hydroamination of isoprene with secondary amines.

of the solvents and reaction conditions are also important. Isoprene and *N*-methylaniline were reacted in 1:1 stoichiometry with 95% selectivity in MeOH using PdCl₂-PPh₃ as catalyst (the overall yield was ca. 60%) [25]. Isoprene reacted with diethylamine in the presence of Pd complex of tris(2,4,6-trimethoxyphenyl) phosphine (cone angle 185°) to give the 2:1 head-to-head adduct in almost quantitative yield [21]. Furthermore, the presence of a strong Lewis acid (HOTf or BF₃·Et₂O) enhanced the selectivity up to 82% in some cases [24]. Hydroamination of isoprene with secondary amines catalyzed by Pd(acac)₂-P(OBu)₃ system gave the tail-to-tail as the main products [26]. In most cases, high selectivity was not obtained in the mild reaction conditions. Also, longer reaction times were needed to obtain remarkable conversion. The above information encouraged us to synthesize and develop highly selective palladium complexes for the synthesis of practically important alicyclic isoprenoid amines *via* hydroamination using mild reaction conditions. These compounds are important intermediates in fragrance, medicine, and agricultural industries.

2. Results and discussion

2.1. Synthesis and characterization of ligands and metal complexes

A set of Pd(II) complexes containing the ligand 4,5-bis(diphenylphosphino)-9,9-dimethylxanthene (Xantphos) were synthesized. To determine the effect of π -acidity of the ligands on the activity and selectivity of the hydroamination reaction, we prepared chalcogenide derivatives of this ligand. The neutral Pd(II) complexes, [Pd(Xantphos)Cl₂] (I), [Pd(Xantphos=O)Cl₂] (II), [Pd(Xantphos=S)Cl₂] (III) and [Pd(Xantphos=Se)Cl₂] (IV), synthesized from [PdCl₂(COD)] (COD=1,5-cyclooctadiene) and corresponding xantphos or xantphos chalcogenide were isolated as air stable complexes in quantitative yields, 98%, 96%, 94% and 93%, respectively (see Scheme 2). Mixture of dichloromethane and tetrahydrofuran was chosen as the solvent. Analytical data can be found in Table 1.

The palladium complexes I, II, III and IV all exhibit a singlet in the ³¹P{¹H} NMR spectra in the range 22.4–48.6 ppm, which are in a similar range to the chemical shifts reported for the palladium complexes containing bidentate phosphines (see Table 2).

Upon substitution of the chalcogenide Xantphos, the resonances due to the phosphorus atom in the ³¹P{¹H} NMR spectra shifted significantly to the highfield. The ³¹P{¹H} NMR spectrum for II (oxide derivative) exhibited a singlet at 48.6 ppm while the singlet

Table 1

Analytical and physical data for Xantphos derivatives and their Pd complexes.

Compound	Color (% yield)	Melting point (°C)
Xantphos = O	White powder (91)	167–171
Xantphos = S	Pale yellow crystals (88)	221–224
Xantphos = Se	Pale yellow powder (83)	264–269 (December)
Complex II	Orange powder (96)	201–206 (December)
Complex III	Red crystals (94)	240–244 (December)
Complex IV	Deep red powder (93)	289–291 (December)

was observed at 42.5 ppm for the sulfide analog III. Likewise, complex IV (Se derivative) exhibited a singlet at 31.4 ppm and selenium satellites at 33.3 and 29.6 ppm with ¹J_{P-Se} = 749 Hz (Table 2).

The IR spectra of the complexes II, III and IV exhibit higher frequencies for the P=X (X=O, S and Se) bands than the free ligands (1175, 641 and 549 compared to 1169, 625 and 535 cm⁻¹), respectively.

2.2. X-ray crystallographic analyses

Crystallographic data and selected bond lengths (Å) and angles (°) are listed in Tables 3 and 4, respectively. C₄₀H₃₃Cl₃OP₂S₂ (Xantphos=S·CHCl₃; Structure 1) crystallizes as colorless blocks in the monoclinic space group C2/c (No. 15) with four molecules in the unit cell (see Fig. 1).

Structure 1 consists of [Xantphos=S] ligand with one chloroform solvated molecule (Fig. 1). The P–S bond distance is 1.944(9) Å, consistent with the range observed for similar phosphine sulfide compounds [27,28]. The unit cell-packing diagram of the ligand is presented in Fig. S1. Some weak hydrogen bonds exist in the structure which may stabilize the crystal packing. One of these hydrogen bonds exists between the H atom of the C–H bond of the solvated chloroform and the S atom of the phosphine sulfide moiety (C21–H21...S1 = 2.942 Å and C21–H21–S1 angle of 134.4°) and another one exists between the C–H bond of a phenyl ring and the Cl atom of the free chloroform molecule (C8–H8...Cl1 = 2.878 Å and C21–H21–S1 angle of 140.6°). Notably, the chloroform molecule is disordered as can be seen in Fig. 1.

Complex I ([Pd(Xantphos)Cl₂]·CH₂Cl₂; Structure 2) consists of one bidentate chelating Xantphos ligand and crystallizes as orange blocks in the triclinic space group P $\bar{1}$ (No. 2) with two molecules in the unit cell. The molecular structure containing atom numbering scheme is shown in Fig. 2. The complex has a distorted square planar geometry. The wide bite angle of the ligand can be the main factor accounting for this geometry. The average Pd–P and Pd–Cl bond distances for complex I (structure 2) are 2.3(2) and 2.33 Å, respectively, and are in agreement with the values reported for similar structures [29].

There are also a number of hydrogen bonds in complex I (structure 2), which are between the THF and dichloromethane free molecules, coordinated chloride atom of the complex, and C–H bonds of phenyl rings, C45–H45A...Cl1ⁱ = 2.81 Å and C44–H45A–Cl1ⁱ

Table 2

³¹P NMR chemical shifts (δ ppm)^a of ligand molecules, Xantphos chalcogenides, and their Pd(II) complexes.

Compound	δ (ppm)	Compound	δ (ppm)
Xantphos = O	56.5	Complex II	60.2 ^d
Xantphos = S	39.7	Complex III	42.5
Xantphos = Se	31.4 ^b	Complex IV	36.2 ^e
Complex I	22.4 ^c		

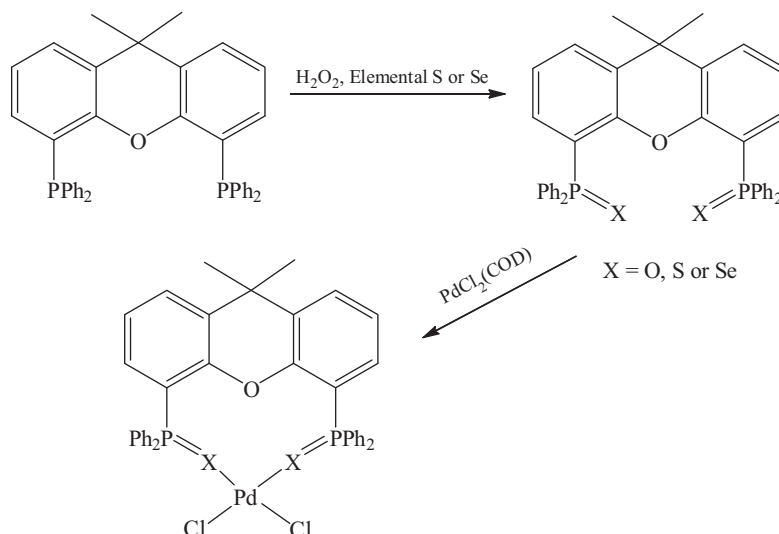
^a Referred to 85% H₃PO₄ as external standard in CDCl₃ solution.

^b ¹J_{P-Se} = 749 Hz.

^c Ref. [29].

^d In DMF-*d*₇ solution.

^e ¹J_{P-Se} = 790 Hz.



Scheme 2. Synthetic procedures for preparation of palladium: Xantphos chalcogenide catalysts.

Table 3
Crystallographic and structure refinements data of Xantphos = S, complexes (I) and (III).^a

Compound	Xantphos = S	Complex I	Complex III
Formula	C ₄₀ H ₃₃ Cl ₅ OP ₂ PdS ₂	C ₄₄ H ₄₂ Cl ₄ O ₂ P ₂ Pd	C ₄₀ H ₃₄ Cl ₄ OP ₂ PdS ₂
Formula weight	762.09	912.94	904.95
Crystal system	Monoclinic	Triclinic	Triclinic
Space Group	C2/c	P $\bar{1}$	P $\bar{1}$
a/Å	12.919(3)	10.564 (2)	11.9136 (3)
b/Å	17.840(4)	11.985 (2)	12.2522 (2)
c/Å	16.546(3)	16.401 (3)	16.1724 (4)
α/°	90	76.77 (3)	94.0480 (14)
β/°	103.86(3)	89.56 (3)	110.0800 (11)
γ/°	90	87.31 (3)	116.3920 (12)
Volume/Å ³	3702.4(15)	2019.2 (7)	1914.90 (7)
Z	4	2	2
Density (calc.)/g cm ⁻³	1.367	1.502	1.569
θ ranges for data collection	2.1–29.2	2.6–17.6	2.7–27.5
F(000)	1576	932	916
Absorption coefficient/mm ⁻¹	0.479	0.84	0.99
Index ranges	–17 ≤ h ≤ 17 –24 ≤ k ≤ 24 –22 ≤ l ≤ 20	–13 ≤ h ≤ 13 –15 ≤ k ≤ 15 –18 ≤ l ≤ 21	–15 ≤ h ≤ 15 –15 ≤ k ≤ 15 –20 ≤ l ≤ 21
Data collected	14524	18899	30920
Unique data (R _{int})	3413, (0.038)	4884, (0.077)	7263, (0.044)
Parameters, restraints	234, 1	480, 0	453, 0
Final R ₁ , wR ₂ ^a (Obs. data)	0.085, 0.1404	0.1654, 0.2642	0.0481, 0.0837
Final R ₁ , wR ₂ ^a (All data)	0.0535, 0.1273	0.0846, 0.2126	0.0350, 0.0773
Goodness of fit on F ² (S)	1.02	1.05	1.03
Largest diff peak and hole/e Å ³	0.53, –0.38	1.68, –1.49	0.86, –0.59

^a $R_1 = \sum ||F_o| - |F_c|| / \sum |F_o|$, $wR_2 = [\sum (w(F_o^2 - F_c^2)^2) / \sum w(F_o^2)^2]^{1/2}$.

Table 4
Selected bond distances (Å) and angles (°) for Xantphos = S, complexes (I) and (III).

Xantphos = S		Complex(I)		Complex(III)	
S1–P1	1.9444 (9)	Cl1–Pd1	2.3341(19)	Pd1–S2	2.0074(9)
P1–C7	1.815 (2)	Cl2–Pd1	2.330(2)	Pd1–Cl2	2.0074(9)
P1–C14	1.815 (2)	Pd1–P1	2.293(2)	Pd1–S1	2.0074(9)
P1–C1	1.825 (2)	Pd1–P2	2.307(2)	Pd1–Cl1	2.0074(9)
Cl1–C21	1.901 (3)	C1–P1	1.816 (7)	Cl3–C1S	2.0074(9)
Cl2–C21	1.635 (4)	C8–P1	1.838 (8)	Cl4–C1S	2.0074(9)
		C35–P2	1.830 (7)	S1–P1	2.0074(9)
		C29–P2	1.826 (7)	S2–P2	2.0074(9)
C7–P1–S1	114.27 (8)	P1–Pd1–P2	100.92 (7)	S2–Pd1–Cl1	87.23 (3)
C14–P1–S1	116.72 (8)	P1–Pd1–Cl2	167.91 (7)	S2–Pd1–S1	86.37 (2)
C1–P1–S1	111.99 (8)	P2–Pd1–Cl2	84.80 (7)	Cl2–Pd1–S1	172.07 (3)
		P1–Pd1–Cl1	85.46 (7)	S2–Pd1–Cl1	174.33 (2)
		P2–Pd1–Cl1	168.37 (7)	Cl2–Pd1–Cl1	89.39 (3)
		Cl2–Pd1–Cl1	87.20 (7)	S1–Pd1–Cl1	96.60 (2)
				P1–S1–Pd1	109.99 (3)
				P2–S2–Pd1	108.09 (3)

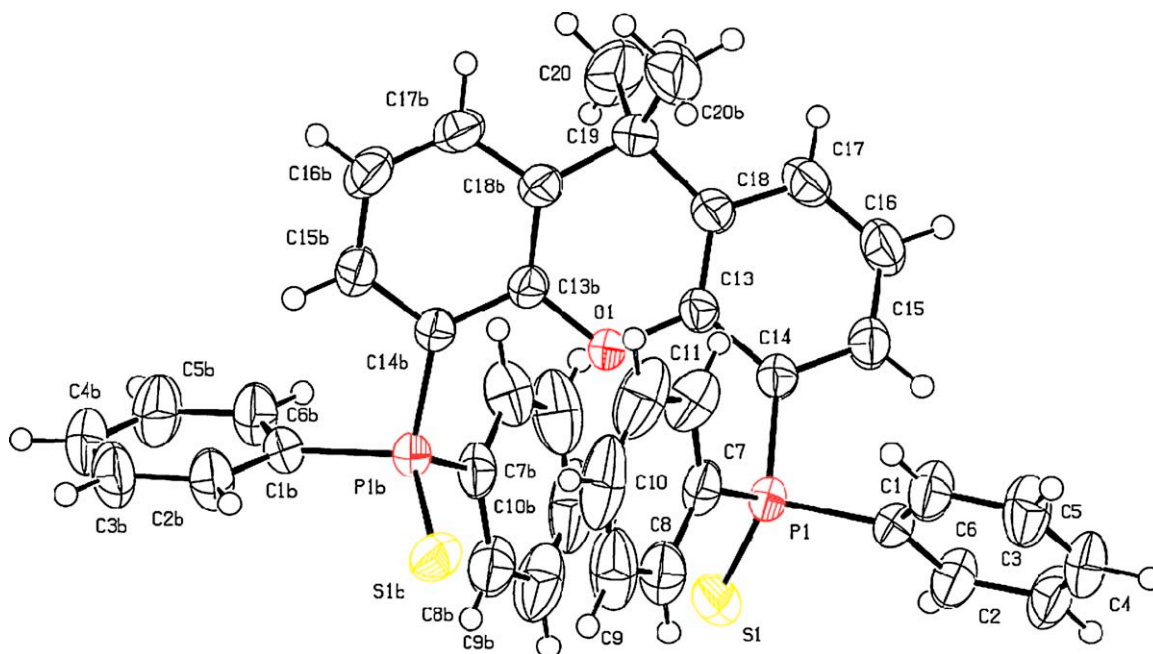


Fig. 1. ORTEP drawings of ligand Xantphos=S with atomic numbering scheme. The thermal ellipsoids are drawn at the 50% probability level at 298 K and disordered chloroform solvated molecule was omitted for more clarity.

with an angle of 160° , $C25-H25...Cl2^{ii} = 2.74 \text{ \AA}$ with an angle of $C25-H25-Cl2^{ii} = 167.0^\circ$ and $C16-H16...Cl1 = 2.72 \text{ \AA}$ with an angle of $C16-H16-Cl1^i = 164.0^\circ$ (symmetry codes: $i = -x, -y + 1, -z + 1$ and $ii = -x, -y + 1, -z$). Packing diagram of complex I can be found in Fig. S2 in supplemental material of this paper.

Complex III, $[\text{Pd}(\text{Xantphos}=\text{S})\text{Cl}_2] \cdot \text{CH}_2\text{Cl}_2$; structure **3** crystallizes as red plates in the triclinic space group $P\bar{1}$ (No. 2) with two molecules in the unit cell (see Fig. 3). Structure **3** is

analogous to structure **2** with xantphos sulfide instead of xantphos, and a distorted square planar configuration around the palladium center. The average Pd–S, Pd–Cl and P–S bond distances for **3** are 2.303(7), 2.308(7) and 2.008(9) Å, respectively, and are in agreement with the values reported previously for palladium phosphine sulfide complexes [30]. Longer P–S bond distance can be attributed to the coordination of the S atoms to the Pd metal core.

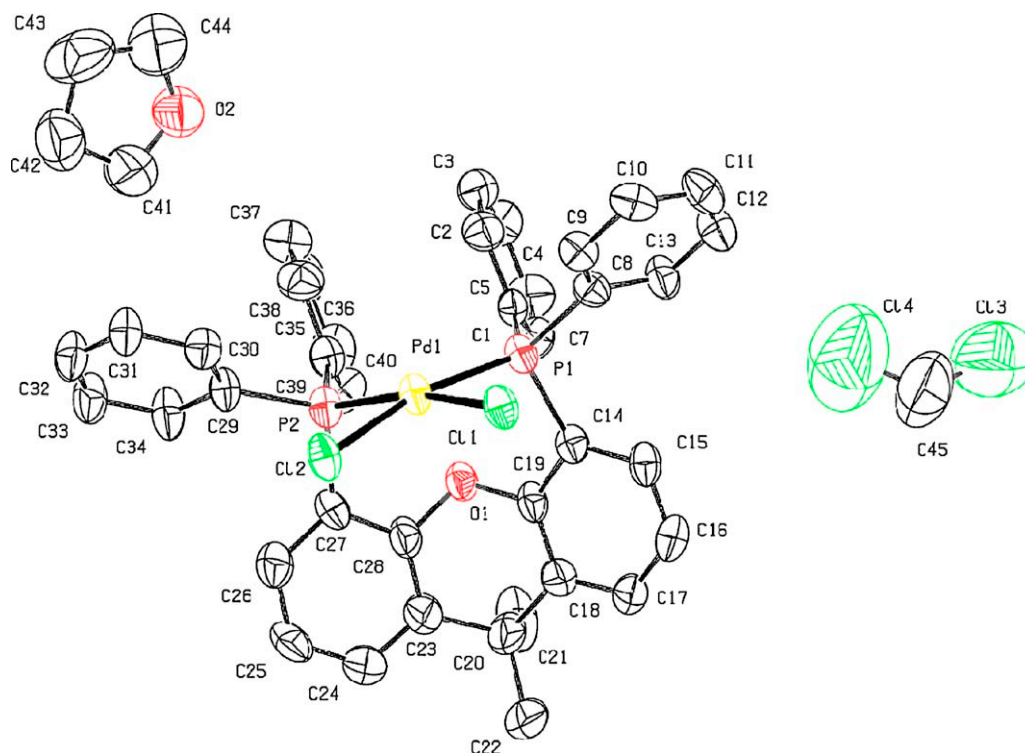


Fig. 2. The molecular structure of complex I, showing atom numbering scheme of complex $[\text{PdCl}_2(\text{Xantphos})]$. The thermal ellipsoids are drawn at the 40% probability level at 293 K. Hydrogen atoms were omitted for clarity.

Table 5
Hydroamination of isoprene with morpholine in various solvents using complex **I** as the catalyst.

Catalyst	Solvent ^a	Time (h)	Conversion (%) ^b	Total selectivity of butylamine (%) ^c	Selectivity of octylamines (%)
[PdCl ₂ (Xantphos)]	MeOH	12	91%	79%	12%
	EtOH	12	94%	81%	13%
	MeCN	12	96%	90%	6%
	DMF	12	82%	68%	14%
	DMSO	12	74%	56%	18%
	Benzene	12	67%	58%	9%
	Toluene	12	73%	62%	11%

^a All reactions were performed at reflux temperature of the corresponding solvent.

^b Conversion of morpholine based on GC analyses.

^c Total selectivity of butylamines.

Similarly, there are a number of hydrogen bonds in complex **III** (structure **3**), which are between the solvated dichloromethane molecules, coordinated chloride atom of the complex, and C–H bonds of phenyl rings. Hydrogen bonds of C1S–H1SB–Cl1 = 2.57 Å and C1S–H1SB–Cl1 with an angle of 156°, C44–H44A···Cl2 = 2.61 Å with an angle of C44–H44A–Cl2 = 149.0° and C34–H34A···Cl2 = 2.79 Å with angle of C34–H34A–Cl2 = 141.0° (symmetry codes: A = x, y, z) are found in the packing of Structure **3** which may stabilize the unit cells (See Fig. S3). Besides, crystal structure packing dominates by C–H···π interactions between neighboring molecules (C23–H23A···Cg1 = 2.827 Å, Cg1 being the ring C54/C53/C52/C51/C56/C55, with A = x, y, z, see Fig. S3, Supplemental Materials).

2.3. Catalytic hydroamination of isoprene

The isoprene hydroamination with a wide range of secondary amines in the presence of the catalytic system, Pd(Xantphos/Xantphos chalcogenide)Cl₂, occurred homogeneously in acetonitrile as reaction solvent. Even though the excess amount of isoprene complicated the processing and characterization of the products, it resulted in the enhancement of conversion, and selectively produces mono-octadienyl amines (see Scheme 1), so we performed the reaction with two equivalents of isoprene.

Palladium catalyzed hydroamination of isoprene with morpholine to give 4-(2-methylbut-2-enyl)morpholine by Takahashi

et al. [26] was not sufficiently effective even at high temperature (140–146 °C) and long reaction time. Another competitive reaction was happened simultaneously to produce 4-(3-methylbut-2-enyl)morpholine in low yield of 16% before reduction with LiAlH₄.

We succeeded to hydroaminate isoprene with secondary amines in the presence of Pd catalysts consisting of Xantphos/Xantphos chalcogenide ligands with improved conversion up to 69% and with high regioselectivity up to 93% for hindered secondary amines. In order to find the optimum conditions for hydroamination reactions, some attempts were made to investigate the effects of solvent and catalyst loading. At first, hydroamination of isoprene with morpholine in the presence of complex **I**, [Pd(Xantphos)Cl₂], as a model substrate was carried out in various solvents such as alcohols, acetonitrile, DMF and DMSO. The reactions were run with molar ratio of 1–2:100:200 for catalyst:amine:isoprene. This ratio was found to be the optimum condition. The reaction was followed by reduction of the produced 2-buteneamine to the corresponding aliphatic amines as described in experimental section.

The hydroamination reaction proceeded at 82 °C (boiling point of MeCN) within 8–12 h and led to the formation of 4-(2-methylbut-2-enyl)morpholine in 78% selectivity and ~95–100% amine conversion (prior to reduction with LiAlH₄). The molar ratio of catalyst and reagents was 1.5–2:100:200 for catalyst:amine:isoprene, respectively. The yield of unsaturated octadienylamines was negligible and essentially depended on the solvent character. The

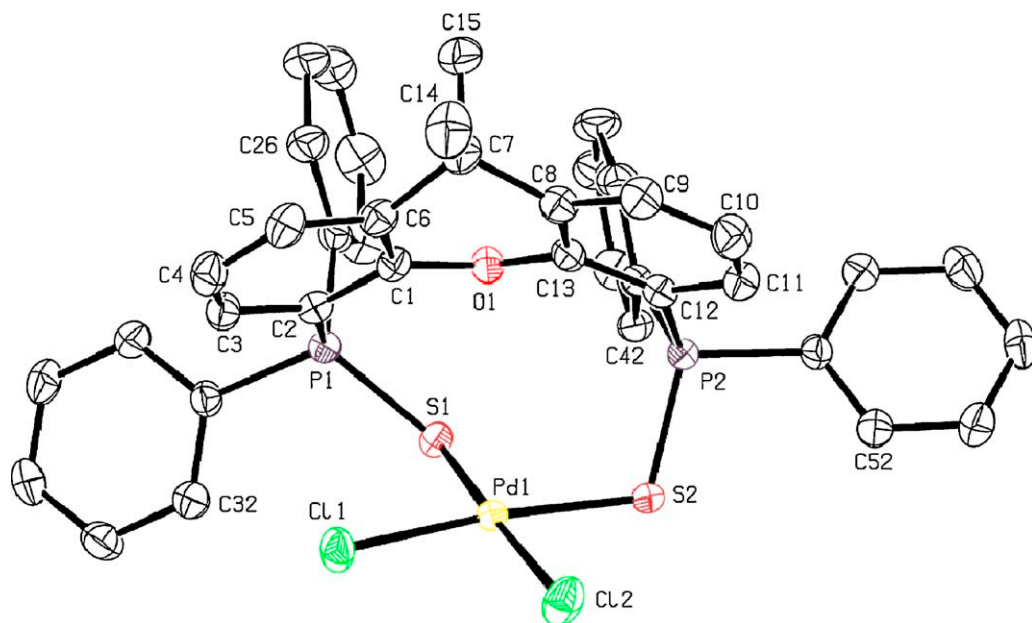
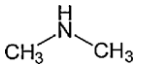
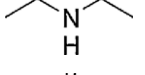
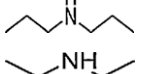
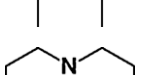
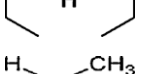
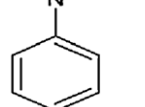
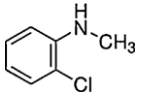
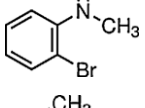
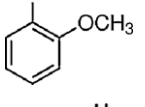
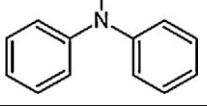


Fig. 3. The molecular structure of complex **III**, showing atom numbering scheme of complex [PdCl₂(Xantphos=S)]. The thermal ellipsoids are drawn at the 50% probability level at 150 K. Hydrogen atoms and dichloromethane solvated molecule were omitted for clarity.

Table 6
Oxidation of a wide range of alcohols using Pd(II) complexes of Xantphos/Xantphos chalcogenides as catalyst in water at room temperature.^{a,b,c}

Entry	Amine	PdCl ₂ (COD)		Complex I		Complex II		Complex III		Complex IV	
		Conv. (%)	Sel. (%)	Conv. (%)	Sel. (%)	Conv. (%)	Sel. (%)	Conv. (%)	Sel. (%)	Conv. (%)	Sel. (%)
1		96	72:17	~100	79:18	96	68:19	97	72:16	99	76:17
2		94	79:11	~100	81:16	94	79:11	95	80:12	97	82:14
3		94	81:10	94	73:17	93	70:14	91	70:12	93	75:10
4		91	71:12	96	78:12	95	71:15	91	73:15	93	75:14
5		83	68:10	92	80:8	93	73:11	88	76:7	90	79:9
6		79	41:29	91	21:67	76	17:53	89	16:66	90	13:73
7		89	14:67	92	13:76	78	14:61	92	15:77	94	9:81
8		87	16:63	90	15:71	75	20:49	88	18:66	92	10:80
9		72	17:52	88	15:70	76	15:53	77	16:53	84	13:65
10		73	11:56	80	17:54	71	15:49	72	13:54	82	14:62
11		79	11:63	82	13:62	74	14:52	71	13:52	79	13:61
12		80	18:51	85	12:69	81	13:61	76	12:61	84	14:64
13		75	12:56	76	9:59	73	10:57	71	11:57	79	10:63

^a Isoprene:Amine:Catalyst (200:100:2) were stirred in a N₂-filled 10 mL stainless steel thermo-regulated (electric oven) autoclave with a glass liner and a magnetic bar.

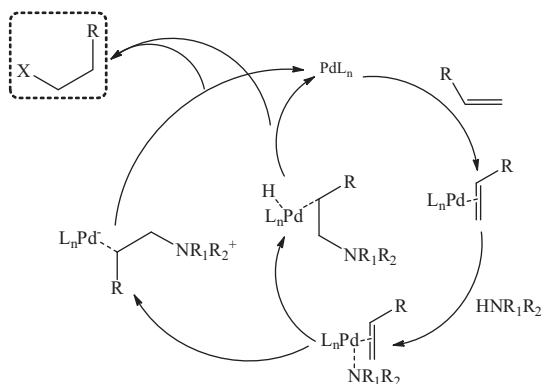
^b The conversion was calculated based on amine substrate, by using GC and with comparison of authentic samples.

^c Selectivity (%) [2-methyl-N,N-dialkyl/arylbutan-1-amine]:[N,N-dialkyl/aryl-3-methylbutan-2-amine].

hydroamination with secondary amines was clean and effective in alcoholic solvents (MeOH and EtOH) or acetonitrile. However, the conversion of the amines was not quantitative in alcohols.

Under same conditions, the higher yield of the unsaturated octadienylamine (14–18%) in hot DMF or DMSO may be due to coordination of the solvent to Pd center and deactivation of the catalyst (see Table 5). At such temperatures, dimerization of the isoprene can occur conveniently and hydroamination reaction becomes

unfavorable. In aromatic solvents such as benzene or toluene, the yield of octadienylamines was lower (9–11%) than aprotic polar solvents (DMF or DMSO), however the amine conversion was not quantitative (67–73%). Moreover, the reaction time was strongly influenced by the reaction temperature. When reaction temperature was maintained at reflux, the reaction completed in 8 h. At lower temperature (40–50 °C) the reaction rate decreased five times (~36–40 h), and concurrently the selectivity of the process



Scheme 3. Proposed reaction pathways for hydroamination of isoprene via intramolecular or intermolecular attack.

was reduced by the formation of a mixture of adducts. The yield of target butylamines decreased to 24–59%.

To study the applicability of the prepared catalysts, hydroamination of isoprene with a wide range of secondary amines were carried out to obtain the saturated butylamines (see Table 6). The reactivity and conversion were dependent on the nature of the amines as well as the catalyst substitute. In the case of stronger bases (lower pK_b of the base), higher conversion of the amine was observed (see Table 6, Entries 1, 2, 4 and 5). Also, amines with higher steric hindrance could be converted to the corresponding 1-isopentylamines with high selectivity. In these cases, 1-isopentylamines were obtained in higher percentages compared to the reactions with lower steric hindrance amines, which were led to 2-methyl-buteneamines before reduction with $LiAlH_4$ (1-(2-methylbutyl) amines after reduction). As we used $LiAlH_4$ in our reduction step, we could not recover our Pd complexes, competently. Most of the Pd in complexes precipitated as Pd black. To resolve this economic problem, we are testing direct reduction of our alkenylamine products by hydrogenation in the presence of Pd catalysts.

Concerning the influence of amine reactants on the reaction, amines with higher basicity react more efficiently. Pyrrolidine and piperidine with $pK_a = 11.26$ and 11.22 respectively [31], showed higher activity and quantitative conversion under our hydroamination conditions. Diethylamine and dimethylamine showed more reactivity while dibutylamine and diisopropylamine had minimum conversion amongst selected secondary amines despite their higher basic character. This may be due to the higher steric hindrance of their alkyl/aryl chains (*iso*-propyl and butyl). On the other hand, such bases produced 1-isopentylamine as the major product in high selectivity. Remarkably, amines with less steric hindrance yield 1-isopentylamines.

Correspondingly, the ligand type has remarkable effect on the catalyst efficiency. As can be seen in Tables 5 and 6, the best conversion as well as the most selectivity was obtained from complex I ($[Pd(Xantphos)Cl_2]$). According to the proposed catalytic cycle (see Scheme 3), Xantphos P-donor ligand may leave the palladium center easier at the first stage rather than leaving its chalcogenides. Higher activity of selenide derivative could be ascribed to the same reason, as well. It is clear that oxygenated phosphine species have least efficiency and selenide phosphine species were more capable toward hydroamination of isoprene. It should be noted that selenide derivative has lower activity compared to complex I ($[Pd(Xantphos)Cl_2]$). Moreover, we run sets of reactions with *N*-methyl-aniline, its chloro, bromo and methoxide derivatives as well as diphenylamine. These amines react slightly lower than aliphatic secondary amines, may be due to the aromatic system of the phenyl ring and participating of the unpaired electrons on the N atom.

Electron withdrawing substituents (Cl and Br) on *N*-methyl-aniline moiety had lower activities might be owing to the electron withdrawing effect on the N atom. On the contrary, electron donating group OMe had more reactivity toward isoprene. All of the secondary aromatic amines preferred position 4 in isoprene which has lower steric hindrance.

3. Conclusion

Anti-Markovnikov regioselective hydroamination of isoprene by Pd–Xantphos/Xantphos chalcogenide system, especially for pyrrolidine and piperidine, were observed in mild conditions ($80^\circ C$, 8 h) with high yields. A regular correlation was observed between the reactivity of the amine and its basicity as well as its steric hindrance. After reduction of the initial buteneamines by $LiAlH_4$, total yield of hydroamination products with secondary amines were increased. We investigated the $PdCl_2(COD)$ complex as catalyst. The complex showed lower activity than all of the four complexes tested in this research. So, the catalytic property depends on presence of phosphine/phosphine Chalcogenides system. $PdCl_2(COD)$ complex was efficient only for pyrrolidine and piperidine amines which have the highest basicity among the tried amines. Catalytic activity of Pd complexes with chalcogenides of Xantphos decreased with increasing electronegativity of the substituent on the phosphorus atom. Notably, electron withdrawing groups on aromatic amines as well as steric hindrance of them can affect reactivity of the amine substrates. It should be mentioned that in the course of isoprene hydroamination experiments some dimerization/oligomerization reactions compete with hydroamination, which is extremely dependent on the reaction time and the temperature as well as the solvent type and the catalyst selectivity.

4. Experimental

4.1. Instrumentation, methods and materials

Complex I ($[Pd(Xantphos)Cl_2] \cdot CH_2Cl_2$), $Pd(COD)Cl_2$ and 4,5-bis(diphenylphosphino)-9,9-dimethylxanthene (Xantphos) were prepared according to the previously published methods [29,32,33]. PPh_2Cl , butyl lithium (15% solution in hexane), elemental S and red Se, H_2O_2 (35% aqueous solution) and the solvents were purchased from Merck and Fluka. The solvents were analytical grade, and were purified and deoxygenated prior to use based on standard methods. Isoprene was dried over CaH_2 , distilled under N_2 at atmospheric pressure, and the fraction distilled at $32^\circ C$ was collected and stored under N_2 at $-15^\circ C$. Melting points are uncalibrated and were measured with an Electrothermal 9200 melting point apparatus. IR spectra from 250 to 4000 cm^{-1} of solid samples were taken from 1% dispersions in CsI pellets using a Shimadzu-470 spectrometer. 1H and ^{31}P NMR spectra were recorded at room temperature on a Bruker AVANCE 500 MHz spectrometer. The NMR spectra are referenced to TMS (1H NMR) and $85\% H_3PO_4$ (^{31}P NMR). Elemental analyses were performed using a Heraeus CHN–O Rapid analyzer. The course of the reactions was monitored by gas chromatography (Agilent Technologies 7890A Instrument), equipped with a capillary column (DB–5, 5% phenyl methyl siloxane, capillary $60\text{ m} \times 0.25\text{ mm I.D.} \times 0.25\ \mu\text{m}$). The samples were collected periodically for analyses with an off-line GC equipped with a mass selective detector (MSD, Agilent 5975C). Peaks were identified on the basis of the mass spectra by matching to a library of NIST spectra. GC/FID was used to determine the concentrations of products in the samples. Catalytic experiments were conducted in an N_2 -filled 10 mL flask with a magnetic stirring bar.

4.2. Preparation of *xantphos*=O

Xantphos (1.15, 2 mmol) was dissolved in THF (50 mL) and excess amount of 3% H₂O₂ was added gently with cooling in an ice bath. The mixture was stirred for an additional 1 h at RT and then the reaction mixture was filtered through Büchner funnel to separate the white precipitate. Crystallization from hot ethanol:THF (5:1) afforded pure *Xantphos* oxide as a white powder (91% yield). *mp* = 164–171 °C. Anal. calcd. for: C₃₉H₃₂O₃P₂: C, 76.71; H, 5.28; found: C, 76.9; H, 5.4. NMR (CDCl₃): ¹H (500 MHz): δ (ppm) = 1.76 (s, 6H); 6.95 (m, 2H); 7.16 (d, 2H); 7.39 (m, 6H); 7.46 (m, 6H); 7.61 (d, 2H); 7.77 (m, 8H). ³¹P: δ (ppm) = 56.5 (s). IR (Csl)/cm⁻¹: 1173 (ν P–O).

4.3. Preparation of *xantphos*=S

Xantphos (1.15 g, 2 mmol) was dissolved in toluene (50 mL) and was mixed with elemental sulfur (0.13 g, 4.05 mmol) and refluxed overnight under dried N₂. Evaporation of the solvent under vacuum afforded crude sulfide derivative. Crystallization from hot chloroform yielded pure *Xantphos* sulfide as colorless block crystals suitable for X-ray crystallography (88% yield). *mp* = 221–224 °C. Anal. calcd. for: C₄₀H₃₃Cl₃OP₂S₂: C, 63.04; H, 4.36; found: C, 63.2; H, 4.4. NMR (CDCl₃): ¹H (500 MHz): δ (ppm) = 1.71 (s, 6H); 6.88 (m, 2H); 7.12 (d, 2H); 7.43 (m, 12H); 7.59 (d, 2H); 7.78 (m, 8H). ³¹P: δ (ppm) = 39.7 (s). IR (Csl)/cm⁻¹: 619 (ν P–S).

4.4. Preparation of *xantphos*=Se

Xantphos (1.15 g, 2 mmol) was dissolved in toluene (50 mL) and was mixed with elemental red selenium (0.32 g, 4.05 mmol) and refluxed overnight under dried N₂. Filtration of the reaction mixture and evaporation of toluene by rotary evaporator afforded crude selenide derivative. Crystallization from hot benzene yielded pure *Xantphos* selenide as a pale yellow powder (83% yield). *mp* = 264–269 °C (December). Anal. calcd. for: C₃₉H₃₂OP₂Se₂: C, 63.60; H, 4.38; found: C, 63.9; H, 4.5. NMR (CDCl₃): ¹H (500 MHz): δ (ppm) = 1.69 (s, 6H); 6.89 (m, 2H); 7.04 (d, 2H); 7.36 (m, 6H); 7.41 (m, 6H); 7.61 (d, 2H); 7.77 (m, 8H). ³¹P: δ (ppm) = 31.4 (s). Satellites were observed for ⁷⁷Se (Natural abundance = 7.63%) at 33.3 and 29.6 ppm (¹J_{P–Se} = 749 Hz). IR (Csl)/cm⁻¹: 533 (ν P–Se).

4.5. Preparation of [PdCl₂(*Xantphos*=O)].THF; complex II

To a solution of *Xantphos*=O ligand, (0.1 g, 0.16 mmol) in THF (20 mL), PdCl₂(COD) (0.038 g, 0.16 mmol) in chloroform (15 mL) was added under an atmosphere of N₂. The color of the reaction mixture changed from pale yellow to light orange. After stirring for 30 min at 50 °C, the volume of the reaction mixture was reduced to ca. 5 mL by rotary evaporator and then freshly distilled Et₂O (20 mL) was added. The resulting precipitate was filtered off and washed with cold diethyl ether (10 mL) and finally dried over P₂O₅. Recrystallization from mixture of THF: EtOH afforded the analytically pure complex (96% yield). *mp* = 201–206 °C (December). Anal. calcd. for: C₄₃H₄₀Cl₂O₄P₂Pd: C, 60.05; H, 4.69; found: C, 60.2; H, 4.7. NMR (DMF *d*₇): ¹H (500 MHz): δ (ppm) = 1.73 (s, 6H); 1.95 (m, 4H); 3.69 (dd, 4H); 7.03 (m, 2H); 7.22 (d, 2H); 7.48 (m, 6H); 7.52 (m, 6H); 7.67 (d, 2H); 7.78 (m, 8H). ³¹P: δ (ppm) = 60.2 (s). IR (Csl)/cm⁻¹: 1165 (ν P–O).

4.6. Preparation of [PdCl₂(*Xantphos*=S)].CHCl₃; complex III

To a solution of *Xantphos*=S ligand, (0.1 g, 0.15 mmol) in chloroform (10 mL), PdCl₂(COD) (0.043 g, 0.15 mmol) was added in chloroform (15 mL) under N₂ atmosphere. The color of the reaction mixture changed from light yellow to deep orange upon addition

of the ligand. After stirring for 30 min at 50 °C, the volume of the reaction mixture was reduced to ca. 5 mL by rotary evaporator and then freshly distilled Et₂O (25 mL) was added. The resulting precipitate was filtered off and washed with cold diethyl ether (10 mL) and finally dried over P₂O₅. Recrystallization from mixture of THF: EtOH afforded the analytically pure complex (94% yield). *mp* = 240–244 °C (December). Anal. calcd. for: C₄₀H₃₃Cl₅OP₂PdS₂: C, 51.14; H, 3.54; found: C, 51.2; H, 3.6. NMR (CDCl₃): ¹H (500 MHz): δ (ppm) = 1.70 (s, 6H); 6.57 (m, 2H); 6.89 (d, 2H); 7.40 (m, 12H); 7.45 (d, 2H); 7.57 (m, 8H). ³¹P: δ (ppm) = 42.5 (s). IR (Csl)/cm⁻¹: 611 (ν P–S).

4.7. Preparation of [PdCl₂(*Xantphos*=Se)].CHCl₃; complex IV

In darkness and under N₂ atmosphere, a solution of *Xantphos*=Se ligand, (0.1 g, 0.14 mmol) in hot chloroform (15 mL) was added to a solution of PdCl₂(COD) (0.039 g, 0.14 mmol) in same solvent (15 mL). The color of the reaction mixture changed immediately from yellow to deep red. After stirring for 30 min at 50 °C, the volume of the reaction mixture was reduced to ca. 5 mL by rotary evaporator and then freshly distilled Et₂O (25 mL) was added. The resulting red precipitate was filtered off and washed twice with cold diethyl ether (2 × 15 mL) and finally dried over silica gel in darkness. Recrystallization from mixture of THF: EtOH afforded the analytically pure complex (93% yield). *mp* = 289–291 °C (Dec.). Anal. calcd. for: C₄₀H₃₃Cl₅OP₂PdS₂: C, 51.14; H, 3.54; found: C, 51.2; H, 3.6. NMR (CDCl₃): ¹H (500 MHz): δ (ppm) = 1.63 (s, 6H); 6.77 (m, 2H); 6.84 (d, 2H); 7.19 (m, 12H); 7.26 (s, 1H); 7.41 (d, 2H); 7.48 (m, 8H). ³¹P: δ (ppm) = 36.2 (s); satellites were observed at 38.4 and 34.5 ppm (¹J_{P–Se} = 790 Hz). IR (Csl)/cm⁻¹: 529 (ν P–Se).

4.8. General procedure for the hydroamination of isoprene

All hydroamination reactions were performed in an N₂-filled 10 mL flask with a magnetic stirring bar. A solution of the catalyst (0.02 mmol, 0.02 equiv.), isoprene (2.0 mmol, 2.0 equiv.), and the secondary amine (1 mmol, 1 equiv.) dissolved in MeCN (5 mL) were charged by cannulation techniques. After refluxing the mixture for required time, the reaction mixture was allowed to cool to room temperature. For reduction of prepared alkene amines a slurry of LiAlH₄ (1.5 mmol, 1.5 equiv.) in dry Et₂O (5–10 mL) was added. This mixture was stirred at room temperature overnight under an atmosphere of N₂. Quenching of reaction mixture performed by slow addition of water (0.1 mL), then 1 M NaOH (0.1 mL), and a further aliquot of water (0.3 mL). After filtration, the solvents were removed under reduced pressure. Column chromatography (hexane: Et₂O, SiO₂) afforded the purified amine products either as single compound or as a mixture of regioisomers. Characterization of the products was done by NMR.

Supplementary data

Supplementary data associated with this article can be found in the online version of the article. CCDC numbers 856776–856778 contains the supplementary crystallographic data for *xantphos*=S and complex I and complex III. These data can be obtained free of charge via <http://www.ccdc.cam.ac.uk/conts/retrieving.html>, or from the Cambridge Crystallographic Data Center, 12 Union Road, Cambridge CB2 1EZ, UK; fax: +44 1223 336 033; or e mail: deposit@ccdc.cam.ac.uk.

Acknowledgements

The authors gratefully acknowledge the financial support from the University of Tehran. Also, we are thankful to Dr. Alan J. Lough from the University of Toronto for crystal structure determinations.

Appendix A. Supplementary data

Supplementary data associated with this article can be found, in the online version, at <http://dx.doi.org/10.1016/j.apcata.2012.05.018>.

References

- [1] M. Rodriguez-Zubiri, S. Anguille, J.J. Brunet, *J. Mol. Catal. A: Chem.* 271 (2007) 145–150.
- [2] M. Nobis, B. Driessen-Hoelscher, *Angew. Chem. Int. Ed.* 40 (2001) 3983–3985.
- [3] R. Severin, S. Doye, *Chem. Soc. Rev.* 36 (2007) 1407–1420.
- [4] J.J. Brunet, N. Châu Chu, O. Diallo, E. Mothes, *J. Mol. Catal. A: Chem.* 198 (2003) 107–110.
- [5] J.J. Brunet, N. Châu Chu, O. Diallo, S. Vincendeau, *J. Mol. Catal. A: Chem.* 240 (2005) 245–248.
- [6] T. Joseph, G.V. Shanbhag, D.P. Sawant, S.B. Halligudi, *J. Mol. Catal. A: Chem.* 250 (2006) 210–217.
- [7] M. Beller, C. Breindl, M. Eichberger, C.G. Hartung, J. Seayad, O.R. Thiel, A. Tillack, H. Trauthwein, *Synlett.* (2002) 1579–1594.
- [8] R. Pryadun, D. Sukumaran, R. Bogadi, J.D. Atwood, *J. Am. Chem. Soc.* 126 (2004) 12414–12420.
- [9] R.O. Ayinla, T. Gibson, L.L. Schafer, *J. Organomet. Chem.* 696 (2011) 50–60.
- [10] D.V. Vitanova, F. Hampel, K.C. Hultsch, *J. Organomet. Chem.* 696 (2011) 321–330.
- [11] D.F. Kennedy, B.A. Messerle, S.L. Rumble, *New J. Chem.* 33 (2009) 818–824.
- [12] L.D. Field, B.A. Messerle, K.Q. Vuonga, P. Turner, *Dalton Trans.* (2009) 3599–3614.
- [13] C. Li, R.K. Thomson, B. Gillon, B.O. Patrick, L.L. Schafer, *Chem. Commun.* (2003) 2462–2463.
- [14] A. Hu, M. Ogasawara, T. Sakamoto, A. Okada, K. Nakajima, T. Takahashi, W. Lina, *Adv. Synth. Catal.* 348 (2006) 2051–2056.
- [15] K.D. Hesp, M. Stradiotto, *Chem. Cat. Chem.* 2 (2010) 1192–1207.
- [16] M. Kawatsura, J.F. Hartwig, *J. Am. Chem. Soc.* 122 (2000) 9546–9547.
- [17] L.K. Vo, D.A. Singleton, *Org. Lett.* 6 (2004) 2469–2472.
- [18] U. Nettekoven, J.F. Hartwig, *J. Am. Chem. Soc.* 124 (2002) 1166–1167.
- [19] M. Kawatsura, J.F. Hartwig, *Organomet.* 20 (2001) 1960–1964.
- [20] M. Utsunomiya, J.F. Hartwig, *J. Am. Chem. Soc.* 125 (2002) 14286–14287.
- [21] S.M. Maddok, M.C. Finn, *Organomet.* 19 (2000) 2684–2689.
- [22] J. Kiji, S. Nishimura, S. Yoshikawa, E. Sasakawa, J. Furukawa, *Bull. Chem. Soc. Jpn.* 47 (1974) 2523–2525.
- [23] C.R. Enzell, I. Wahlberg, A.J. Aasen, *Wien.* (1977).
- [24] W. Keim, M. Röper, M. Schieren, *J. Mol. Catal.* 20 (1983) 139–151.
- [25] L.I. Zakharkin, E.A. Petrushkina, *Izv. Akad. Nauk SSSR, Ser. Khim.* (1986) 1344–1347.
- [26] K. Takahashi, A. Miyake, C. Hata, *Bull. Chem. Soc. Jpn.* 45 (1972) 1183–1191.
- [27] A. Nemati Kharat, A. Bakhoda, T. Hajiashrafi, A. Abbasi, *Phosphorus Sulfur* 185 (2010) 2341–2347.
- [28] D.C. Apperley, N. Bricklebank, M.B. Hursthouse, M.E. Light, S.J. Coles, *Polyhedron* 20 (2001) 1907–1913.
- [29] A.M. Johns, M. Utsunomiya, C.D. Incarvito, J.F. Hartwig, *J. Am. Chem. Soc.* 128 (2006) 1828–1839.
- [30] S. Aizawa, T. Hase, T. Wada, *J. Organomet. Chem.* 692 (2007) 813–818.
- [31] H.K. Hal, *J. Am. Chem. Soc.* 79 (1957) 5441–5444.
- [32] D. Drew, J.R. Doyle, *Inorg. Synth. R. J. Angelici.* 28 (1990) 345.
- [33] M. Kranenburg, Y.E.M. van der Burgt, P.C.J. Kamer, P.W.N.M. van Leeuwen, K. Goubitz, J. Fraanje, *Organomet.* 14 (1995) 3081–3089.